

Arabidopsis halleri shows hyperbioindicator behaviour for Pb and leaf Pb accumulation spatially separated from Zn

Stephan Höreth^{1*}, Paula Pongrac^{1,2*} , Johannes T. van Elteren³ , Marta Debeljak³, Katarina Vogel-Mikus^{2,4} , Michael Weber¹ , Manuel Braun¹, Björn Pietzenuk⁶ , Matic Pečovnik² , Primož Vavpetič² , Primož Pelicon² , Iztok Arčon^{2,5} , Ute Krämer⁶  and Stephan Clemens^{1,7} 

¹Department of Plant Physiology, University of Bayreuth, 95440 Bayreuth, Germany; ²Jožef Stefan Institute, 1000 Ljubljana, Slovenia; ³National Institute of Chemistry, 1000 Ljubljana, Slovenia; ⁴Biotechnical Faculty, University of Ljubljana, 1000 Ljubljana, Slovenia; ⁵University of Nova Gorica, 5000 Nova Gorica, Slovenia; ⁶Molecular Genetics and Physiology of Plants, Ruhr University Bochum, 44801 Bochum, Germany; ⁷Bayreuth Center for Ecology and Environmental Research, University of Bayreuth, 95440 Bayreuth, Germany

Summary

Author for correspondence:

Stephan Clemens

Tel: +49 921 552630

Email: stephan.clemens@uni-bayreuth.de

Received: 12 June 2019

Accepted: 1 December 2019

New Phytologist (2020) **226**: 492–506

doi: 10.1111/nph.16373

Key words: *Arabidopsis thaliana*, elemental imaging, food webs, metal contamination, metal distribution, metal speciation, metallophyte.

- Lead (Pb) ranks among the most problematic environmental pollutants. Background contamination of soils is nearly ubiquitous, yet plant Pb accumulation is barely understood. In a survey covering 165 European populations of the metallophyte *Arabidopsis halleri*, several field samples had indicated Pb hyperaccumulation, offering a chance to dissect plant Pb accumulation.
- Accumulation of Pb was analysed in *A. halleri* individuals from contrasting habitats under controlled conditions to rule out aerial deposition as a source of apparent Pb accumulation. Several elemental imaging techniques were employed to study the spatial distribution and ligand environment of Pb.
- Regardless of genetic background, *A. halleri* individuals showed higher shoot Pb accumulation than *A. thaliana*. However, dose–response curves revealed indicator rather than hyperaccumulator behaviour. Xylem sap data and elemental imaging unequivocally demonstrated the *in planta* mobility of Pb. Highest Pb concentrations were found in epidermal and vascular tissues. Distribution of Pb was distinct from that of the hyperaccumulated metal zinc. Most Pb was bound by oxygen ligands in bidentate coordination.
- *A. halleri* accumulates Pb whenever soil conditions render Pb phytoavailable. Considerable Pb accumulation under such circumstances, even in leaves of *A. thaliana*, strongly suggests that Pb can enter food webs and may pose a food safety risk.

Introduction

Lead (Pb) is one of the most problematic environmental pollutants, ranking, for example, second on the Agency for Toxic Substances and Disease Registry 2017 substance priority list. The list is based on assessments of frequency, toxicity, and the potential for human exposure at or near hazardous waste sites (<https://www.atsdr.cdc.gov/spl/index.html>). Pb has been anthropogenically released into the environment at least since the invention of cupellation *c.* 5000 yr ago. During the industrial revolution and with the introduction of leaded gasoline in the 1920s, world Pb production rose to several million tons per year. Despite the ban on tetraethyl Pb in gasoline and on the use of Pb in many consumer products since the 1970s, Pb production remains at almost 5 million tons per year according to data compiled by the US Geological Survey (<https://minerals.usgs.gov/minerals/pubs/commodity/lead/>). Widespread Pb pollution results in continuous

low-level exposure of organisms including humans to Pb. For Cd and As it is well documented that they are taken up from the soil as Cd²⁺ and arsenate or arsenite, respectively, into plants and enter food webs in this way (Adriano, 2001; McLaughlin *et al.*, 2011). By contrast, the bioavailability and mobility of Pb in soil is generally very low. K_d values, that is the distribution coefficients between the solid phase of a soil and the pore water, are much (orders of magnitude) higher for Pb than for As and Cd species (Janssen *et al.*, 1997; Sauvé *et al.*, 2000; McLaughlin *et al.*, 2011). Hence, concentrations of ionic Pb in soil solutions are very low. This is predominantly explained by the strong sorption of Pb to soil particles and dissolved organic matter (Degryse *et al.*, 2007). Consequently, when Pb was a major target of early phytoremediation research, chelators were frequently added to the soil in order to improve Pb bioavailability (Huang *et al.*, 1997; Wang *et al.*, 2007; Saifullah *et al.*, 2009).

The Pb that is nonetheless taken up shows very little mobility within a plant, that is the root-to-shoot translocation factors are small (Mohtadi *et al.*, 2012a, 2013). Accordingly, when the

*These authors contributed equally to this work.

relative contribution of uptake from the soil vs aerial deposition to leaf Pb accumulation was analysed, the majority of studies found that most of the Pb in leaves was airborne (McLaughlin *et al.*, 2011; Schreck *et al.*, 2012). Therefore, studies into Pb accumulation have to be performed: (1) under conditions limiting aerial contamination; and (2) should avoid problems arising from the poor Pb bioavailability in frequently used growth media; namely, Pb has a strong propensity to precipitate with phosphate. Thus, plants need to be cultivated in medium with low phosphate concentrations and a pH of 5.0 or below (Sauvé *et al.*, 1998; Kopitke *et al.*, 2008, 2010).

Because of these technical challenges, we know very little about the mechanisms of Pb accumulation in plants. However, we need to understand this, given the ubiquitous presence of Pb as a contaminant in the environment and the potential role of plants in mediating transfer of Pb into food webs (Norton *et al.*, 2014, 2015). Mechanistic insight into biological processes is often facilitated by studying organisms showing maximum rates of the process in question. The most extreme accumulation of nonessential metals or metalloids known in nature is shown by metal hyperaccumulating plants. Metal hyperaccumulation is defined as the accumulation of an element in above-ground organs to a level two to three orders of magnitude larger than in normal plants growing under similar conditions in the natural habitat (Baker, 1981; van der Ent *et al.*, 2013). More than 700 hyperaccumulators have been described to date, most of these being Ni hyperaccumulators (Reeves *et al.*, 2018). The other elements, for which hyperaccumulation was clearly demonstrated in much smaller numbers of species, include zinc (Zn), Cd, copper (Cu), manganese (Mn), chromium (Cr), selenium (Se) and arsenic (As) (Krämer, 2010; van der Ent *et al.*, 2013; Pilon-Smits, 2017; White & Pongrac, 2017). There are also studies in the literature on Pb (hyper)accumulation, that is leaf concentrations in field samples exceeding the Pb hyperaccumulation threshold of $1000 \mu\text{g g}^{-1}$ dry weight (DW) (Vogel-Mikuš *et al.*, 2005; Pongrac *et al.*, 2007; Koubová *et al.*, 2016; Mahdavian *et al.*, 2016; Dinh *et al.*, 2018). However, they have met scepticism given the possible local contamination by dust, soil particles and aerosols, especially when plants were sampled in the vicinity of Pb sources (van der Ent *et al.*, 2013).

In a large field survey covering the distribution range of the facultative metallophyte and metal hyperaccumulation model system *Arabidopsis halleri* (L.) O'Kane & Al-Shehbaz in Europe, leaf Pb concentrations above the hyperaccumulation threshold have been found in several individuals (Stein *et al.*, 2017). The highest recorded values were 2030 and $2025 \mu\text{g Pb g}^{-1}$ DW in two individuals from a metalliferous site near a former Zn smelter in Miasteczko Śląskie, Poland. Overall, leaf Pb accumulation above hyperaccumulation threshold was confined to individuals sampled from metal-contaminated soil in *A. halleri*. Across nearly 2000 leaf–soil data pairs for European *A. halleri* populations, a strong positive correlation was evident between leaf Pb accumulation and BaCl_2 -extractable Pb in the soil. This was in stark contrast to Zn accumulation, which was extremely large in most individuals independent of soil exchangeable Zn. Cd accumulation varied strongly, but was found also on soils with low

Cd availability (Stein *et al.*, 2017). Therefore, careful analysis of Pb accumulation under controlled conditions in the laboratory is required to exclude potential aerial deposition.

In light of the need to understand Pb accumulation by plants, we explored Pb translocation mechanisms and Pb deposition in *A. halleri*. To this end, plants of selected *A. halleri* accessions and *Arabidopsis thaliana* (L.) Heynh. Col-0 were grown under standardised conditions: (1) in contaminated soil derived from a metalliferous *A. halleri* site, (2) in soil with varying metal contamination to establish dose–response relationships, and (3) in hydroponic culture specifically designed to allow precise control over available Pb^{2+} . In order to gain first insights into Pb accumulation mechanisms, Pb concentrations in roots, leaves and in xylem sap were determined. Candidate genes for Pb uptake were identified from RNA-seq data sets and analysed for transcript abundance. Tissue-specific Pb allocation was studied in leaves of the strongest Pb-accumulating *A. halleri* accessions, using laser ablation-inductively coupled plasma-mass-spectrometry (LA-ICP-MS), micro-particle-induced-X-ray emission (micro-PIXE) and scanning electron microscopy with energy dispersive X-ray spectroscopy (SEM-EDX). In addition, the local chemical environment of Pb in *A. halleri* leaves was determined using X-ray absorption near edge structure (XANES) analysis.

Materials and Methods

Plant material and growth conditions

Cuttings of *A. halleri* accessions, originally collected in the field (Supporting Information Fig. S1) and kept in a glasshouse (Stein *et al.*, 2017) with subsequent acclimatisation for 1–5 months in climate chambers (22°C , 16 h light : 8 h dark), were placed in modified 1/10 Hoagland solution ($0.2 \text{ mM } (\text{NH}_4)_2\text{HPO}_4$, $0.4 \text{ mM } \text{Ca}(\text{NO}_3)_2$, $0.6 \text{ mM } \text{KNO}_3$, $0.2 \text{ mM } \text{MgSO}_4$, $5 \mu\text{M } \text{FeCl}_3$, $5 \mu\text{M } \text{HBED}$ (*N,N'*-di(2-hydroxybenzyl)ethylenediamine-diacetic acid monohydrochloride hydrate), $4.63 \mu\text{M } \text{H}_3\text{BO}_3$, $0.032 \mu\text{M } \text{CuSO}_4$, $0.915 \mu\text{M } \text{MnCl}_2$, $0.077 \mu\text{M } \text{ZnSO}_4$, $0.011 \mu\text{M } \text{MoO}_3$), containing 0.3% (w/v) benomyl (Sigma-Aldrich) for 2–3 wk to allow root development. Cuttings with uniform root length (2–4 cm) were used for all the subsequent experiments.

Soil experiments

For the Pb accumulation experiment, soil from the contaminated site Bestwig ($51^\circ 18' 22.20''\text{N}$, $8^\circ 24' 34.80''\text{E}$; average total Pb $8403 \mu\text{g g}^{-1}$, total Zn $9980 \mu\text{g g}^{-1}$, total Cd $22 \mu\text{g g}^{-1}$, Stein *et al.*, 2017) was air dried, homogenised and sieved through a 1 cm mesh. To this soil, 50% v/v vermiculite was added. For the Pb gradient experiment, this Bestwig-soil-vermiculite mixture was further diluted with a 2 : 1 mixture of mineral soil and sand to attain the following treatments (presence of contaminated soil): 0%, 2.5%, 5%, 10%, 20% and 100%. For determining extractable metal concentrations in soil samples, 3 g of air-dried substrate was extracted with 10 ml HCl (1 h at room

temperature) using an overhead shaker at 150 rpm. In order to derive an estimate of phytoavailable metal cations, exchangeable metal was determined via extraction with 10 mM BaCl₂ (Hendershot & Duquette, 1986; Menzies *et al.*, 2007). The extracts were centrifuged for 10 min at 3000 g. Supernatants were collected and stored at 4°C until analysis.

Plants were randomly distributed in a growth chamber (and shifted regularly to avoid position effects) under 50 µmol m⁻² s⁻¹ light (16 h light : 8 h dark) at 22°C. Five replicates of each accession were prepared. At harvest, shoots were cut above the soil level, carefully washed in distilled water and dried using paper towels.

Hydroponic experiments

Cuttings of selected *A. halleri* accessions were transferred to 1.5-l containers (three plants per container) filled with a modified 1/10 Hoagland medium containing only 10% of the initial phosphate concentration (20 µM) and with a pH of 5.0 (Fischer *et al.*, 2014). Half of the containers were supplemented with 5 µM Pb (as Pb(NO₃)₂), while all contained additional 10 µM Zn (added as ZnSO₄). The nutrient solution was changed every 4 d and pH was monitored during the course of the experiments. Three independent experiments were performed with three replicates of each *A. halleri* accession. One reference experiment with six *A. thaliana* Col-0 plants was performed under the same experimental conditions with precultivation of plants to a rosette diameter of 2 cm, approximately matching the shoot biomass of *A. halleri* cuttings at the start of the Pb treatment. At harvest, roots and shoots were separated and root lengths were recorded. Roots were desorbed at 4°C with distilled water (twice 10 min), 20 mM CaCl₂ (once 10 min), 10 mM EDTA (once 10 min). Shoots were carefully washed in distilled water, surface water was removed using paper towels and shoot fresh weight (FW) was recorded. In one experiment, shoots were dissected into petioles, leaf main vein and leaf lamina. All plant material was oven dried at 60°C for 3 d.

Candidate gene identification and transcript analysis

As described in more detail in Methods S1, candidate *cyclic nucleotide gated channels (CNGC)* genes were identified in RNA-seq data sets for the *A. halleri* accessions Laut-3 and Wall-7. Coding sequences were reconstructed from RNA-seq reads and transcript abundance analysed by qRT-PCR (Methods S1).

Xylem sap collection and GC-MS analysis

Plants were cut 1 cm above the root–shoot transition zone and xylem was collected for a total period of 4 h using a micropipette and stored at –20°C until further analysis. Collected volumes averaged 86 ± 46 µl per plant with no apparent difference between treatments. From each exudate sample, 30 µl was acidified with 270 µl 65% HNO₃, incubated for 10 min at room temperature, filled up to a final volume of 3 ml and kept at 4°C until further analysis. Here, 15 µl of xylem sap were analysed by gas

chromatography-mass spectrometry (GC-MS) as described previously (Cornu *et al.*, 2015).

Sample preparation for localisation analyses

Mature leaves were selected from three individual plants and a small piece (*c.* 5 × 2 mm) of the petiole and of the leaf, comprising the main vein with the adjunct leaf lamina, was taken from the lower half of the leaf. Samples were cryo-fixed, cryo-sectioned and freeze dried as described previously (Vogel-Mikuš *et al.*, 2014). For the LA-ICP-MS analysis, cross-sections were deposited on a piece of precooled Parafilm and localisation mapping was performed as described previously (Ilunga Kabeya *et al.*, 2018). For detailed LA-ICP-MS operating conditions and data analysis see Methods S1. For the micro-PIXE analysis, cross-sections were sandwiched between two Pioloform foils stretched over custom-made aluminium frames. Micro-PIXE mapping was performed as described previously (Klančnik *et al.*, 2014). The micro-PIXE spectra were analysed and quantitative distribution maps were generated using the GEOPIXE II software package (Ryan, 2000). Distribution maps were filtered using smooth (Gaussian function, standard deviation = 1.5) and edge enhance (Roberts function) filters in GeoPIXE II.

For the SEM-EDX analysis, pieces of mature leaves were plunge-frozen in liquid propane (KF 80; Universal Cryofixation Unit, Reichert-Jung, Despey, NY, USA) and freeze dried for 3 d at –20°C and 0.210 mbar and analysed using a calibrated energy dispersive X-ray fluorescence microprobe (JXA-8200; Jeol, Tokyo, Japan).

Local chemical environment of Pb

Pb L₃-edge XANES spectra were recorded at the beamline BM23 of the European Synchrotron Radiation Facility (ESRF, Grenoble, France) as described previously (Pongrac *et al.*, 2016). Fresh leaves were frozen in liquid nitrogen and analysed in fluorescence detection mode at 80 K. Reference Pb complexes (Pb-acetate, Pb-cellulose, Pb-chloride, Pb-citrate, Pb-cysteine, Pb-glutathione, Pb-histidine, Pb-malate, Pb-pectin, Pb-sulfate and Pb-sulfide) were recorded in transmission detection mode at room temperature. The Pb-phosphate spectrum was obtained from Shen (2014). The resolution of the monochromator in the region of the Pb L₃-edge was 2 eV and the absolute energy reproducibility of the measured spectra was ±0.05 eV. The absorption spectra were measured within the interval from –150 to 250 eV relative to the Pb L₃-edge at 13 035 eV. In the XANES region, equidistant energy steps of 0.5 eV were used. The Pb L₃-edge XANES spectra were analysed using the IFEFFIT program package ATHENA (Ravel & Newville, 2005).

Inductively coupled plasma-optical emission spectroscopy (ICP-OES)

Oven-dried plant material was wet digested using 3 ml 65% HNO₃ (w/w) in a microwave (STarT 1500; MLS GmbH, Leutkirch im Allgäu, Germany) by ramping for 20 min to 180°C

Table 1 BaCl₂- and HCl-extractable concentrations ($\mu\text{g g}^{-1}$ DW) of lead (Pb), zinc (Zn) and cadmium (Cd) of differently diluted contaminated soil (Bestwig).

Proportion of contaminated soil		0%	2.5%	5%	10%	20%	100%
Proportion of control laboratory soil		100%	97.5%	95%	90%	80%	0%
BaCl ₂	Pb	0.05	0.06	0.06	0.11	0.27	1.28
	Zn	0.1	0.3	0.5	1.5	6.4	42.8
	Cd	nd	nd	0.01	0.02	0.06	0.42
HCl	Pb	5.46	165	440	713	1481	5676
	Zn	11	51	88	162	1161	5970
	Cd	0.06	0.19	0.56	0.94	2.89	11.39

The dilutions were prepared with control laboratory soil to generate the gradient of metal concentrations in the substrate as indicated.

and holding for 10 min. After cooling to room temperature, samples were filled up to 10 ml with 2% HNO₃ for subsequent analysis. Element concentrations in this wet-digested plant material, in soil extracts and in the xylem sap were determined using an iCAP 6500 Duo (Thermo Scientific, Waltham, MA, USA).

Statistical analysis

In order to determine accession effects on element and biomass responses, a one-way analysis of variance (ANOVA) was conducted, followed by the Tukey post-hoc test at $P < 0.05$ while, for pairwise comparisons, differences were tested using Student's *T*-test at $P < 0.05$ in SIGMAPLOT v.13.0 (Systat Software, San Jose, CA, USA).

Results

Accumulation of Pb by *Arabidopsis halleri* in contaminated soil

In a large-scale field study, several *A. halleri* individuals had been identified as putative Pb hyperaccumulators (Stein *et al.*, 2017). Because all of these were sampled at contaminated sites impacted by mining or metal smelting activities, the Pb (hyper)accumulation potential was tested here under controlled laboratory conditions to exclude aerial deposition of Pb as the underlying cause for high Pb concentrations. Selected accessions representing metallicolous (M) and nonmetallicolous (NM) populations as well as different biogeographic regions (Fig. S1) were grown for 6 wk in native soil from a contaminated *A. halleri* site in Bestwig (Germany). This soil contained BaCl₂-extractable metal at concentrations of 1.28 $\mu\text{g Pb g}^{-1}$, 42.8 $\mu\text{g Zn g}^{-1}$ and 0.42 $\mu\text{g Cd g}^{-1}$, and HCl-extractable metal at concentrations of 5676 $\mu\text{g Pb g}^{-1}$, 5970 $\mu\text{g Zn g}^{-1}$ and 11.4 $\mu\text{g Cd g}^{-1}$ (Table 1). At harvest, the leaves of all accessions contained high levels of Pb (Fig. 1). The origin of a given accession, that is M or NM site, did not affect the leaf Pb concentrations significantly. Average Pb concentration in accessions from M sites was 599 $\mu\text{g Pb g}^{-1}$ DW (minimum–maximum range was 376–780 $\mu\text{g Pb g}^{-1}$ DW) and from NM sites it was 646 $\mu\text{g Pb g}^{-1}$ DW (range: 300–788 $\mu\text{g Pb g}^{-1}$ DW). All *A. halleri* accessions contained more Pb than the reference plant *A. thaliana* after growth in the same contaminated soil in

the same experiment. The average for *A. thaliana* was 145 $\mu\text{g Pb g}^{-1}$ DW. The lack of correlation between Pb and titanium (Ti) excluded the possibility that the accumulated leaf Pb was the result of contamination with soil particles (Fig. 1d).

By contrast with low variation in Pb concentrations, Zn and Cd concentrations were substantially affected by accession and biogeographic origin. On average, accessions from M sites contained less Zn than accessions from NM sites (8122 $\mu\text{g Zn g}^{-1}$ DW and 17 120 $\mu\text{g Zn g}^{-1}$ DW, respectively) and ranges were larger (Fig. 1b). Still, the lowest Zn concentration measured in *A. halleri* exceeded the Zn concentration in the reference *A. thaliana* Col-0 (495 $\mu\text{g Zn g}^{-1}$ DW) by five times.

While Cd concentrations were nearly as variable as Zn concentrations, the influence of the origin was negligible. Accessions from M soil contained on average 39.5 $\mu\text{g Cd g}^{-1}$ DW (minimal–maximal range was 11.3–90.3 $\mu\text{g Cd g}^{-1}$ DW) and accessions from NM sites 46.7 $\mu\text{g Cd g}^{-1}$ DW (range: 22.9–71.3 $\mu\text{g Cd g}^{-1}$ DW; Fig. 1c). Accumulation of Pb, Zn and Cd did not affect the growth of plants visibly. Accessions differed in average biomass, but overall no difference in ranges was observed between plants from M and NM sites (Fig. S2).

Zinc, Cd and Pb were the only elements, for which leaf concentrations differed between *A. halleri* and *A. thaliana* Col-0. Concentrations of calcium (Ca), potassium (K), magnesium (Mg), phosphorus (P), Cu, iron (Fe) and Mn were all in similar ranges (Fig. S3).

The influence of soil Pb availability on Pb accumulation

A hallmark of hyperaccumulation are high metal concentrations in above-ground tissues even when the soil available metal concentrations are low. Consequently, the leaf–soil element relationship is described by a saturation curve (Baker, 1981; van der Ent *et al.*, 2013). In order to study whether Pb accumulation in *A. halleri* behaved accordingly, plants were grown in M soil from a native *A. halleri* site and in soil step-wise diluted with noncontaminated substrate mixture. Resulting BaCl₂- and HCl-extractable concentrations of Pb, Zn and Cd are shown in Table 1. Two *A. halleri* accessions with the strongest Pb accumulation in the initial soil experiment (one originating from an M site, Laut-3 and one from an NM site, Wall-7) and for comparison the accession with the weakest Pb accumulation, Sieb-1

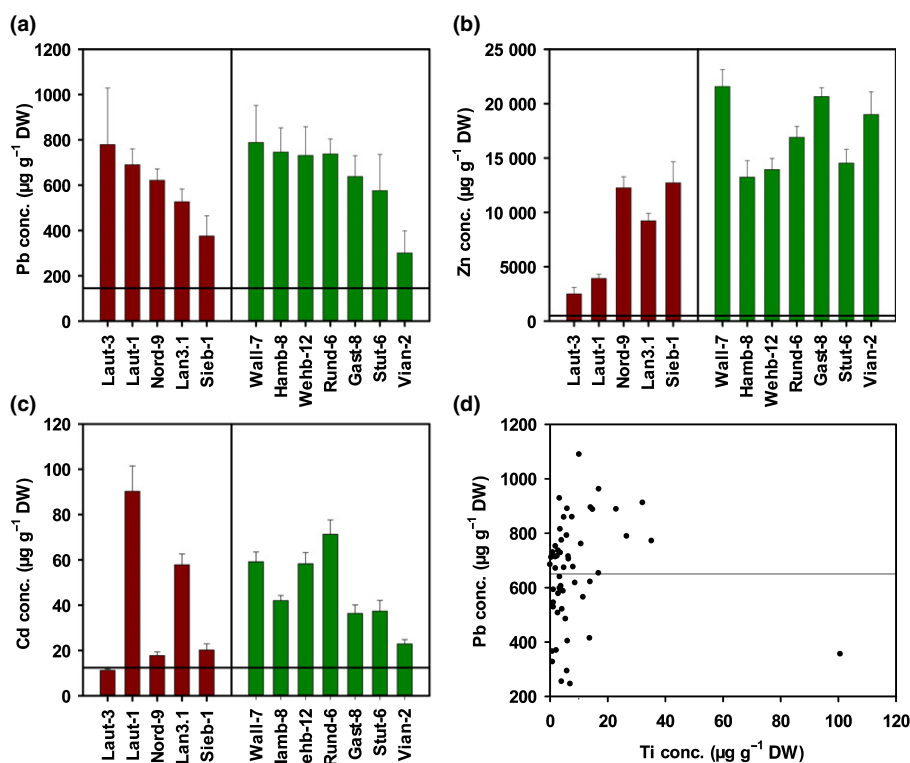


Fig. 1 Metal accumulation in *Arabidopsis halleri* shoots after cultivation in native metalliferous soil. Content of lead (Pb; a), zinc (Zn; b) and cadmium (Cd; c) in shoots of selected *A. halleri* individuals originating from metalliferous (red columns) and nonmetalliferous sites (green columns) grown for 6 wk in metal-rich soil under standardised controlled growth chamber conditions. For names and origin of the individuals see Supporting Information Fig. S1. Values in (a–c) are means ($n = 5$) \pm SD. The horizontal line in (a), (b) and (c) indicates the mean value for *A. thaliana* Col-0 ($n = 5$) grown in the same experiment. (d) Shoot Pb content plotted against titanium (Ti) content to check for contamination by soil particles; DW, dry weight.

(Fig. 1a), were selected for this experiment. As before, *A. thaliana* Col-0 was tested alongside the chosen *A. halleri* accessions. A typical hyperaccumulator response, that is strong accumulation even when soil metal availability was low, was observed for Zn in all three *A. halleri* accessions and for Cd in accessions Wall-7 and Sieb-1 (Fig. 2). By contrast, Pb accumulation showed a nearly linear correlation with HCl-extractable Pb. This was similar to the accumulation behaviour observed in *A. thaliana* Col-0 for all three metals. Plotting shoot element concentrations against BaCl₂-extractable Pb, Zn and Cd in soil yielded essentially the same patterns (Fig. S4).

Possible physiological effects of soil dilution were assessed by analysing biomass and shoot elemental profiles. Overall, growth of the three *A. halleri* accessions was stimulated by the addition of at least a small proportion of native contaminated soil, whereas *A. thaliana* Col-0 showed a slight decrease in growth. Only in undiluted Bestwig soil was *A. halleri* growth negatively affected in one accession (Laut-3) (Fig. S5). Shoot elemental profiles obtained from plants cultivated in the different soil dilutions indicated that macro- and microelement accumulation varied little and concentrations were, in all cases, well above deficiency thresholds (White & Brown, 2010; Fig. S6).

Arabidopsis halleri Pb accumulation in hydroponic culture

To further explore the ability of *A. halleri* to translocate Pb to above-ground tissues, experiments in hydroponic culture were performed. A nutrient solution with low pH and low phosphate was used to prevent precipitation of Pb with phosphate (Fischer *et al.*, 2014) and thus control Pb availability. Indeed, speciation

analysis using VISUALMINTEQ indicated that all added Pb was available (Table S1). After 3 wk of exposure to 5 μM Pb²⁺, root growth inhibition was apparent, with Wall-7 showing the strongest response (Fig. 3). Growth inhibition observed in *A. thaliana* Col-0 was of a similar magnitude (Fig. S7). Nonetheless, Pb concentrations of the three *A. halleri* accessions were 4–12-fold larger than the Pb concentrations measured in *A. thaliana* Col-0 (average of 49 $\mu\text{g g}^{-1}$ DW) (Fig. 4, indicated by a horizontal line). The pattern of variation between *A. halleri* accessions was different from the soil experiments. The largest Pb shoot concentrations after hydroponic cultivation were measured in Sieb-1 (on average 604 $\mu\text{g Pb g}^{-1}$ DW). Root Pb concentrations determined after desorption exceeded 10 000 $\mu\text{g g}^{-1}$ DW and were much higher than Zn concentrations (Fig. 4). Consequently, apparent root-to-shoot translocation factors were much lower for Pb (on average between 0.022 and 0.036) than for Zn (on average between 3.18 and 4.08). As in the soil experiments, variation in shoot Zn concentrations between accessions was more pronounced than variation in Pb concentrations. The order Wall-7 > Sieb-1 > Laut-3 observed in the soil experiments for Zn accumulation was confirmed in hydroponic culture (Fig. 4). Noteworthy, the Laut-3 accession did not contain more Zn than *A. thaliana* in this experiment (see the reference line in Fig. 4). Interestingly, Pb²⁺ exposure caused an overall reduction in shoot Zn concentrations. This was not seen for Fe (Fig. 4) even though generally a decrease in the content of other mineral nutrients was observed in the Pb-treated plants (Fig. S8). The measured concentrations were always in the sufficient range (White & Brown, 2010), indicating that plants were not deficient in any of the essential elements.

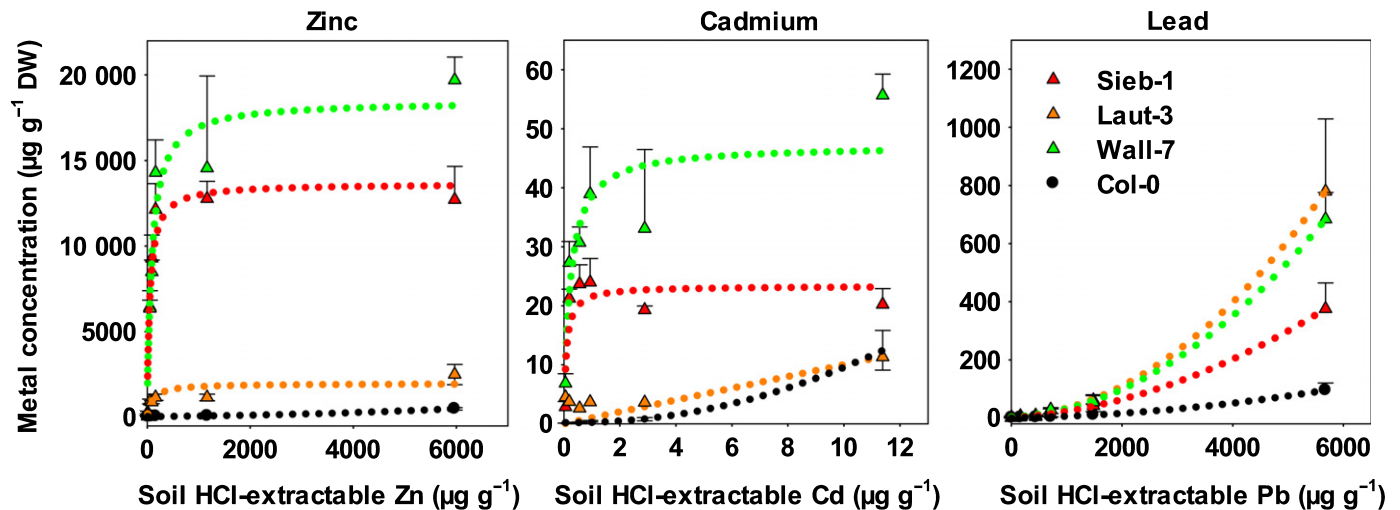


Fig. 2 Shoot metal accumulation depending on soil extractable metal. HCl-extractable zinc (Zn), cadmium (Cd) and lead (Pb) and concentrations of Zn, Cd and Pb were measured in shoots of selected *Arabidopsis halleri* individuals. Sieb-1 (red symbols) and Laut-3 (orange symbols) originated from metalliferous sites, Wall-7 (green symbols) originated from a nonmetalliferous site. Shoot metal content of *A. thaliana* Col-0 grown in different dilutions of metal-rich soil under standardised controlled growth chamber conditions for 6 wk. Values are means ($n = 5$) + SD; DW, dry weight.

To gain first insights into the mechanisms of Pb uptake and accumulation, we performed competition experiments. Analyses of the large field data set for European *A. halleri* populations had indicated that of all analysed soil parameters, Ca had the strongest negative influence on leaf Pb accumulation (Stein *et al.*, 2017). We therefore analysed Pb accumulation in hydroponic culture in the presence of either Ca or Zn excess. Root Pb concentrations of all accessions were strongly reduced in the presence of elevated Ca, whereas Zn excess had practically no effect (Fig. S9). Root Zn concentrations were not affected by extra Ca. Changes in shoot Pb accumulation did not show clear trends. For one accession (Sieb-1), a reduction was observed with high external Ca. For the two other accessions, the opposite effect was seen.

Comparative transcript analysis of candidate Ca^{2+} channel genes

Suppression of root Pb concentrations in the presence of elevated Ca suggested a possible contribution of Ca transporters to Pb uptake. Indirect evidence had implicated CNGCs in *A. thaliana* Pb uptake (Sunkar *et al.*, 2000). To obtain CNGC genes that were candidates for differential expression between *Arabidopsis* species or *A. halleri* accessions, we performed an extrapolating comparison of available results from two different RNA-seq experiments including both roots and shoots of either *A. thaliana* (Col) or the *A. halleri* Laut and Wall populations. *CNGC11* and *CNGC12* were identified as candidate genes based on $\log_2(\text{fold change}) \geq \pm 3$ and adjusted $P < 0.05$ (Table S2). Transcript sequences were reconstructed to generate one consensus per gene for each sequenced replicate and tissue sample, utilising all reads that mapped to the orthologues of each of the *A. thaliana* loci in the *A. halleri* ssp. *gemmaifera* reference genome (see Methods S1). Transcript abundance was analysed in roots and shoots of *A. thaliana* and *A. halleri* plants grown hydroponically under

control conditions. For *CNGC11*, strongly elevated transcript abundance was observed in Laut-3 and Wall-7 relative to Col-0 (Fig. S10). Similar, albeit less pronounced, differences were found for *CNGC12*. This confirmed the RNA-seq results. However, the best Pb-accumulating accession in hydroponic culture, Sieb-1, did not show elevated *CNGC11* or *CNGC12* transcript levels.

Xylem sap element concentrations

Results of the soil and hydroponic experiments showed root-to-shoot translocation of Pb. To investigate this further we obtained xylem sap from hydroponically grown plants. Pb was detected in xylem sap of all three Pb-treated *A. halleri* accessions (Fig. 5). The range of Pb concentrations in the xylem resembled that for Fe, while it was much smaller than Zn, Ca and Mg concentrations. The largest Pb concentration in the xylem was found for the Sieb-1 accession. This was confirmed when data were normalised to Ca concentrations to account for variation in the volume of sampled xylem sap (Fig. S11).

Changes in xylem sap metabolite levels of Pb-accumulating plants may provide information on possible Pb ligands. Therefore, xylem sap samples were subjected to GC-MS analysis. The volcano plot in Fig. S12 summarises the findings. Among the identified metabolites more abundant in Pb-exposed plants was citrate, while GABA and β -alanine were less abundant. For a complete list of metabolite signals detected and quantified see Table S3. Because the xylem sap contains many unknown metabolites, a complete speciation modelling is not possible. In order to nonetheless obtain an estimate as to whether citrate could be a Pb ligand in the xylem, we used element concentrations measured here and known *A. halleri* xylem sap concentrations of citrate and malate (Cornu *et al.*, 2015). The numbers derived for this highly simplified scenario predict *c.* 6–8% of the Pb to be bound by organic acids (Table S4).

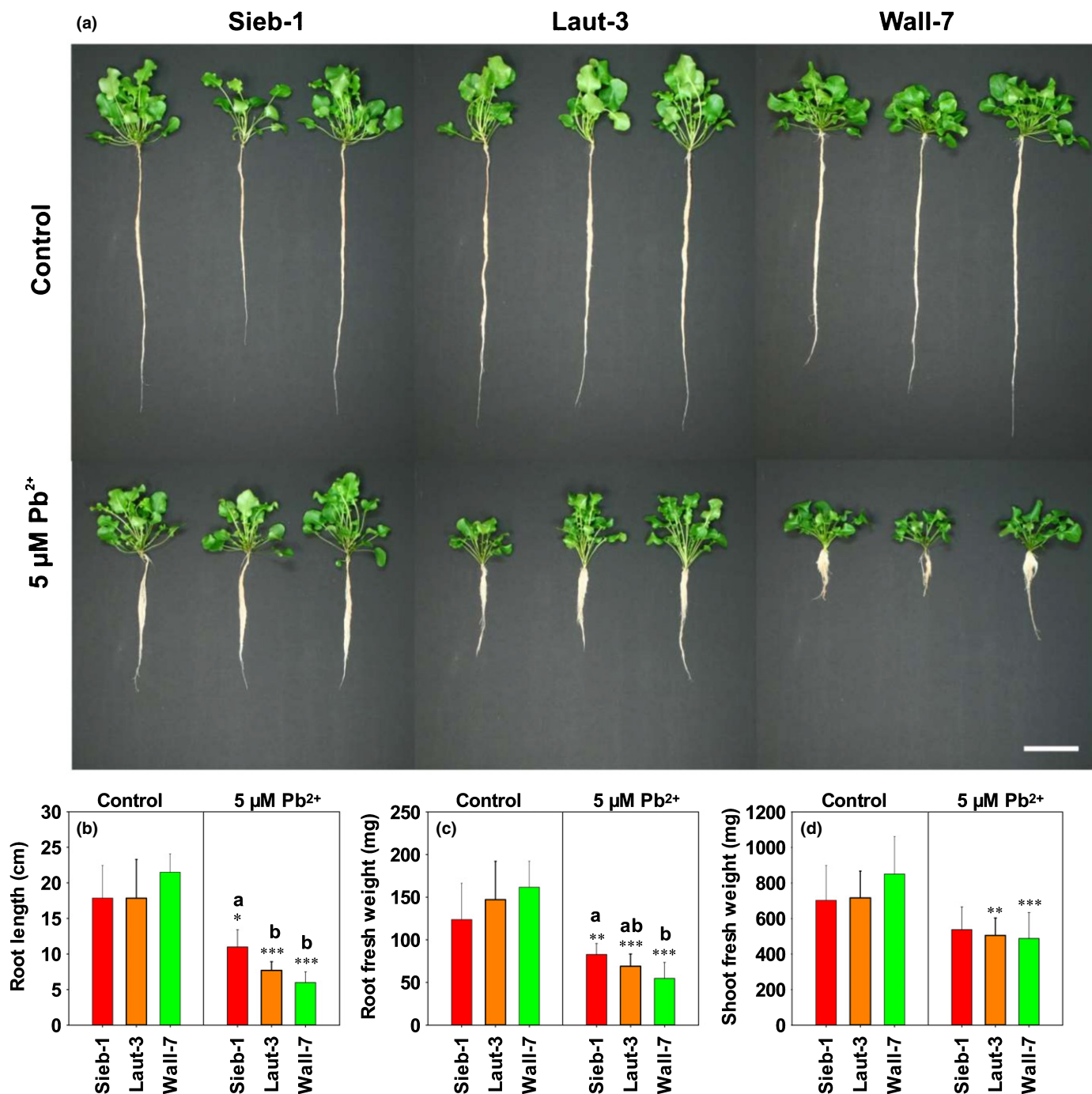


Fig. 3 Growth response of *Arabidopsis halleri* individuals to Pb^{2+} exposure in hydroponic culture. (a) Photographs of whole plants. Bar, 10 cm. (b) Root length, (c) root fresh weight, and (d) shoot fresh weight of selected *A. halleri* individuals, grown hydroponically for 3 wk in a low phosphate, low pH medium in the absence of (Control) or in the presence of $5 \mu\text{M Pb}^{2+}$. Sieb-1 (red bars) and Laut-3 (orange bars) originated from metalliferous sites, Wall-7 (green bars) originated from a nonmetalliferous site. Values in (b–d) are means ($n = 9$) + SD, in which asterisks indicate statistically significant differences between treatments for each accession separately (Student's *t*-test: *, $P < 0.05$; **, $P < 0.01$; ***, $P < 0.001$) and different letters indicate statistically significant differences between accessions in each treatment (one-way ANOVA followed by Tukey honest significant difference (HSD) test at $P < 0.05$).

Tissue-specific distribution of Pb and Zn in *Arabidopsis halleri*

High shoot Pb concentrations and the presence of Pb in xylem sap of *A. halleri* plants exposed to Pb in soil or hydroponic

culture demonstrated translocation of Pb from roots to shoots. We therefore initiated a series of experiments to obtain information on the spatial distribution of Pb in above-ground tissues and on the Pb local chemical environment. Sieb-1 was chosen, as this accession showed strongest Pb accumulation in hydroponic

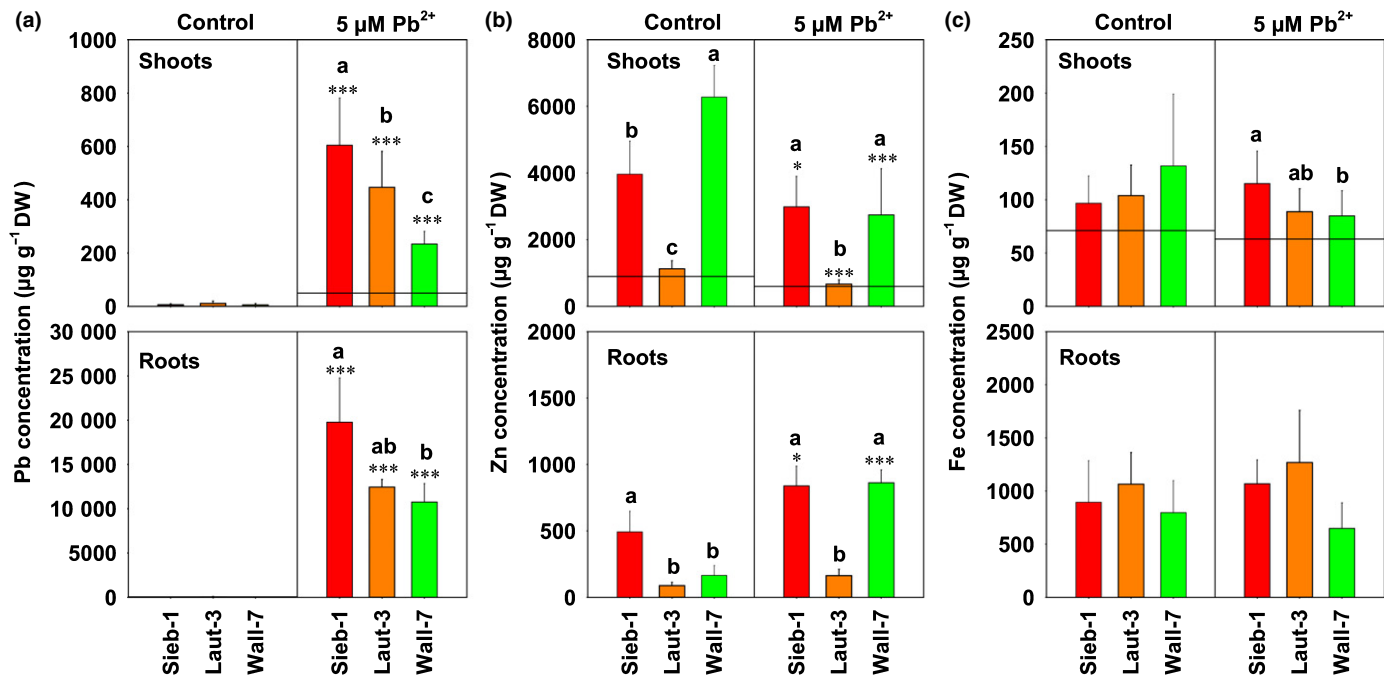


Fig. 4 Metal accumulation in roots and shoots of hydroponically grown *Arabidopsis halleri* and *A. thaliana* plants. (a) Lead (Pb), (b) zinc (Zn) and (c) iron (Fe) content in roots (lower panel) and shoots (upper panel) of selected *A. halleri* individuals and *A. thaliana* Col-0 grown hydroponically for 3 wk in a low phosphate, low pH medium in the absence of (Control) or in the presence of 5 μM Pb^{2+} . Sieb-1 (red bars) and Laut-3 (orange bars) originated from metalliferous sites, Wall-7 (green bars) originated from a nonmetalliferous site. Values are means ($n = 9$) + SD for *A. halleri*. As a reference, average values ($n = 6$) for *A. thaliana* shoots are indicated by a horizontal reference line. Asterisks indicate statistically significant differences between treatments for each accession separately (Student's *t*-test: *, $P < 0.05$; ***, $P < 0.001$) and different letters indicate statistically significant differences between accessions in each treatment (one-way ANOVA followed by Tukey HSD test at $P < 0.05$); DW, dry weight.

culture. First, cross-sections of petioles and leaves were analysed with LA-ICP-MS. In petioles, Pb and Zn distribution maps revealed the allocation of both metals to the epidermis and tissues of the central vascular bundle, whereas in the leaves Pb and Zn allocated to different tissues (Fig. 6). Here, Pb retained the same distribution as in the petiole (epidermis and tissues of central vascular bundle, particularly to xylem and abaxial collenchyma cells), while Zn was preferentially allocated to the parenchyma surrounding the main vein and to the mesophyll of the leaf blade. Line scans across the leaf main vein and the leaf lamina (Fig. 6c, d), averaging three independent distribution maps, further supported these observations. Independent micro-PIXE analyses confirmed the observed distributions of Pb and Zn and provided quantitative distribution maps of Mg, P, S, K and Ca as well (Fig. S13). Surprisingly, both analyses indicated higher Pb concentrations in the petiole than in leaves or leaf tissues. Therefore, an additional hydroponic culture experiment was performed to verify these observations. Indeed, by far the largest Pb concentrations in all three *A. halleri* accessions were measured in the petioles compared with the main leaf vein and the leaf lamina (Fig. S14). By contrast, Zn contents were larger in the main leaf vein and the leaf lamina compared with the petiole, in line with observations from distribution maps.

Trichomes were reported to store extraordinary quantities of Cd and Zn in *A. halleri* (Küpper *et al.*, 2000). Therefore, they were mapped using SEM-EDX to determine localisation of Pb, Cd and Zn in the best Pb-accumulating accession from the soil

experiments (Wall-7). Distribution maps revealed significant allocation of Pb to epidermal cells supporting the trichome, while Zn and Cd were allocated to the base of the trichome (Fig. S15).

Local chemical environment of Pb

To investigate the Pb ligand environment, Pb $L_{3\text{-XANES}}$ spectra were recorded in shoots of two *A. halleri* accessions grown in hydroponic culture. Only oxygen ligands were found for Pb in the first coordination sphere. Linear combination fitting suggested that the majority (68% and 55% for Sieb-1 and Laut-3, respectively) of these oxygen ligands bound Pb in bidentate coordination (determined using the Pb-acetate reference). The remaining Pb ligands have either an octahedral coordination (determined using the PbSO_4 reference) with 16% and 28% for Sieb-1 and Laut-3, respectively, or a monoclinic coordination (determined using the $\text{Pb}_3(\text{PO}_4)_2$ reference; the Space Group $C 1 2/c 1$) with 16% and 25% for Sieb-1 and Laut-3, respectively (Fig. 7).

Discussion

Human activities have over millennia and particularly over the past 150 yr led to a nearly ubiquitous Pb contamination of the Earth's critical zone, that is the surface/near-surface environment that supports life (Marx *et al.*, 2016), making Pb one of the most problematic environmental contaminants. In spite of this

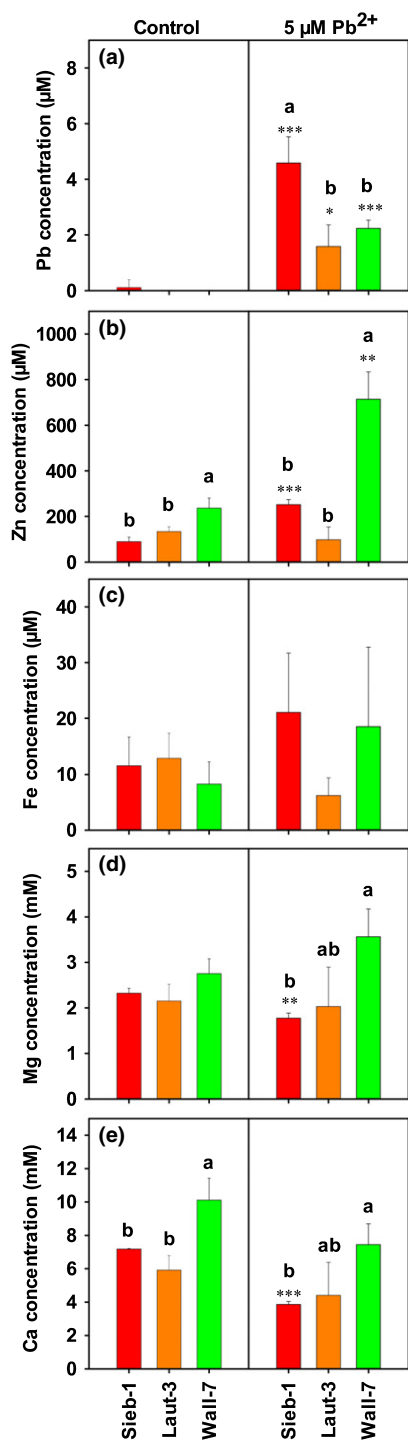


Fig. 5 Element concentrations in xylem sap. (a) Lead (Pb), (b) zinc (Zn), (c) iron (Fe), (d) magnesium (Mg), and (e) calcium (Ca) concentrations in xylem sap sampled from selected *Arabidopsis halleri* individuals grown hydroponically for 3 wk in a low phosphate, low pH medium in the absence of (Control) or in the presence of 5 μM Pb^{2+} . Sieb-1 (red bars) and Laut-3 (orange bars) originated from metalliferous sites, Wall-7 (green bars) originated from a nonmetalliferous site. Values are means ($n = 3$) + SD. Asterisks indicate statistically significant differences between treatments for each accession separately (Student's t -test: *, $P < 0.05$; **, $P < 0.01$; ***, $P < 0.001$) and different letters indicate statistically significant differences between accessions in each treatment (one-way ANOVA followed by Tukey HSD test at $P < 0.05$).

importance, however, little information is available about the movement of Pb into the phytosphere and associated food webs. It has been widely accepted that Pb is poorly mobilised, a consequence of strong Pb soil persistence and poor Pb bioavailability (Zhao *et al.*, 2004; Schreck *et al.*, 2012; Norton *et al.*, 2014, 2015; Fakhri *et al.*, 2018).

The high shoot Pb concentrations observed in the field for a plant with extreme ionic traits such as *A. halleri* offers an opportunity to make inroads into mechanistically understanding Pb accumulation. The ability of *A. halleri* to translocate Pb from the root to the shoot was therefore systematically analysed in controlled Pb exposure experiments. Five main conclusions are drawn from the data: (1) *A. halleri* can indeed strongly accumulate Pb in leaves via translocation from the root; (2) *A. halleri* is not a Pb hyperaccumulator, but rather a Pb bioindicator; (3) there is only limited within-species variation in the Pb accumulation trait, by contrast to the Cd and Zn accumulation; (4) *A. halleri* roots are Pb sensitive regardless of origin, while shoots suffer much less growth inhibition; (5) pathways of Pb accumulation appear to be distinct from pathways of Zn accumulation.

The cultivation of plants on native soil under standardised laboratory conditions arguably offers the best chance to determine metal accumulation traits accurately, devoid of aerial Pb contamination (Mohtadi *et al.*, 2012a,b; Mišljenović *et al.*, 2018). The *A. halleri* field survey had identified a number of samples with high leaf Pb concentrations up to values above the hyperaccumulation threshold of $1000 \mu\text{g g}^{-1}$ DW (Stein *et al.*, 2017). Such an observation had, in the past, often been the only basis to classify a plant as a hyperaccumulator. Soil for our experiments was taken from one of the accessible *A. halleri* sites supporting strong Pb accumulation. Several leaf samples collected in Bestwig showed Pb content above $400 \mu\text{g g}^{-1}$ DW (Stein *et al.*, 2017). When a set of *A. halleri* individuals originating from M and NM sites was cultivated in Bestwig soil, Pb contents between $c. 300$ and $800 \mu\text{g g}^{-1}$ DW were observed (Fig. 1a), confirming the field observations. Importantly, contents of leaf Ti, a soil particle contamination marker (Cook *et al.*, 2009), did not correlate with Pb (Fig. 1d). This indicated true accumulation of Pb via root-to-shoot translocation.

When assessing genotype influence on accumulation behaviour, clear differences were apparent between Zn and Pb. Zn accumulation capacity differs between *A. halleri* accessions from M and NM sites. According to phenotyping data for a large set of genotypes, M individuals show a reduced capacity to hyperaccumulate Zn compared with NM individuals (Stein *et al.*, 2017). Correspondingly, the transcriptomes of M and NM individuals show distinct differences (Schvartzman *et al.*, 2018). Our soil experiments confirmed the pattern for Zn and, at the same time, showed that Pb accumulation behaviour is not associated with the habitat of origin, consistent with minor genotype influence. Rather, our data indicated that whenever Pb is phytoavailable, all *A. halleri* plants can substantially accumulate Pb. This is in line with the strong correlation between available soil Pb and leaf Pb observed in field data (Stein *et al.*, 2017).

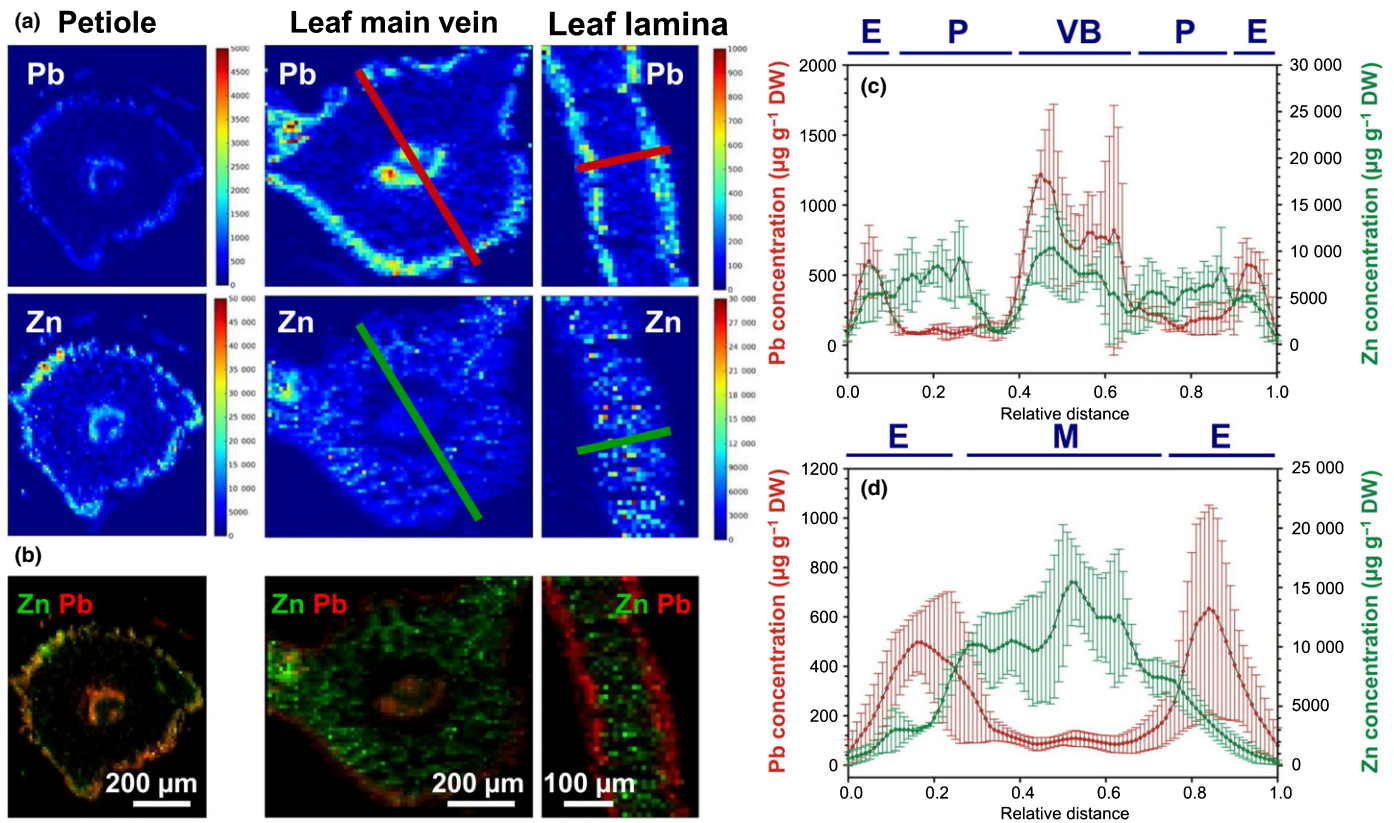


Fig. 6 Spatial distribution of lead (Pb) and zinc (Zn) in leaves of *Arabidopsis halleri*. Representative cross-sections of petiole, leaf main vein and leaf lamina of *A. halleri* individual Sieb-1 grown in hydroponics for 3 wk in the presence of 5 μM Pb²⁺ were analysed by laser ablation-inductively coupled plasma-mass spectrometry. (a) Distribution maps for Pb and Zn. Colour legends indicate concentrations for the two elements (in mg kg⁻¹ dry weight (DW)). (b) Co-localisation maps of Pb (red) and Zn (green). (c, d) Semiquantitative distribution profiles of Pb and Zn across the leaf main vein (c) and leaf lamina (d); E, epidermis, M, mesophyll, P, parenchyma, VB, vascular bundle. Values are averaging three independent cross-sections. Positioning of transects across leaf tissues is indicated in (a) with red (for Pb) and green (for Zn) lines.

A hallmark of metal hyperaccumulation and thus a second criterion to be tested, is a dose–response relationship described by a saturation curve (Baker, 1981). Soil dilution experiments confirmed hyperaccumulation response for Zn and Cd (Figs 2, S4). The expected exclusion-like response described by an exponential curve, which was reported for *Noccaea* (formerly *Thlaspi*) *praecox* Wulfen with the largest Pb content of 740 μg Pb g⁻¹ in leaves (Vogel-Mikuš *et al.*, 2006), was not observed in *A. halleri*. Instead, leaf Pb concentrations in *A. halleri* showed a nearly linear response with HCl-extractable (Fig. 2) as well as BaCl₂-extractable (Fig. S4) soil Pb. The response to soil Pb was clearly different from both hyperaccumulation and exclusion, and demonstrated indicator behaviour. Nonspecific ‘breakthrough’ into shoot tissue due to metal toxicity (Pollard *et al.*, 2014) can be ruled out as there was no reduction in biomass when plants were grown in less diluted soil (Fig. S6). The stronger accumulation relative to other plants cultivated in the same conditions, in this case *A. thaliana* (Fig. 1a), together with indicator-like behaviour, can be described with the term ‘hyperbioindicator’ as proposed for *Gomphrena claussenii* Moq. (Villafort Carvalho, 2016).

Further evidence for true Pb accumulation in *A. halleri* came from hydroponic experiments performed with a medium containing low phosphate and low pH at which Pb²⁺ remains soluble

(Kopittke *et al.*, 2008, 2010; Fischer *et al.*, 2014). To address possible concerns regarding the nutritional status of plants grown in this medium, we analysed leaf ionomes. Although shoot mineral status was perturbed by Pb exposure (Fig. S8), presumably as a result of a competition between Pb and divalent cations for uptake as described in detail for rice (Kim *et al.*, 2002), the contents of macro- and micronutrients remained in sufficiency range. This factor and the absence of nutrient deficiency symptoms indicated the suitability of the hydroponic culture for *A. halleri* plants. After 3 wk of exposure to 5 μM Pb, average concentrations between 230 and 600 μg Pb g⁻¹ DW were detected in leaves of *A. halleri* accessions (Fig. 4). They exceeded the Pb concentrations in *Noccaea jankae* A. Kaern grown in hydroponic solution at 5 μM Pb (Koubová *et al.*, 2016) 8.5-times, and equalled Pb content of *Matthiola flavida* Boiss. grown in hydroponic solution at 5 μM Pb (Heidari Dehno & Mohtadi, 2018). However, translocation factors for Pb were more than two orders of magnitude lower than for Zn as most of the Pb remained in root tissue. This situation further argues against the classification of *A. halleri* as a Pb hyperaccumulator.

Finally, the analysis of xylem sap directly demonstrated Pb mobility inside the plant (Fig. 5). Pb was detected, albeit at much lower concentrations than Zn as expected from the difference in translocation factors. For two out of three accessions, Pb

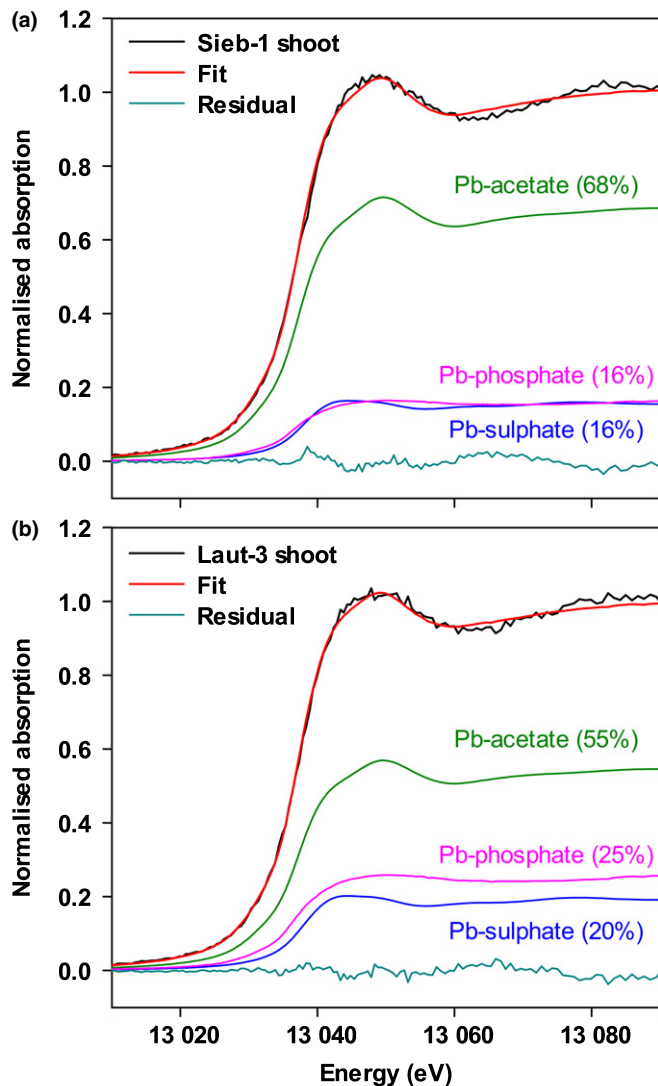


Fig. 7 Lead (Pb) ligand environment in *Arabidopsis halleri*. Pb L_{3} -edge XANES spectra in shoots of Sieb-1 (a) and Laut-3 (b) grown hydroponically for 3 wk in a low phosphate, low pH medium in the presence of $5 \mu\text{M Pb}^{2+}$ and the best linear combination fit ('Fit') obtained by the spectra of the three reference Pb compounds (Pb-acetate, Pb-sulfate and Pb-phosphate). The relative amount of each component is given in parenthesis; eV, electron volts.

treatment appeared to exert a stimulating effect on xylem sap Zn even though overall Zn accumulation in shoots was slightly lower in Pb-exposed plants (Fig. 4). This difference may be due to a difference between an observation for one short time period, that is the xylem sap sampling, and an observation that integrates over the whole cultivation period, that is total shoot Zn.

Interestingly, the concentration of citrate, an important player in Fe long distance transport (Schuler *et al.*, 2012; Álvarez-Fernández *et al.*, 2014) was increased significantly in Pb-treated plants (Fig. S12) and speciation prediction tentatively suggested the formation of Pb-citrate complexes (Table S4). Citrate had been previously observed to respond to Pb treatment in leaves of metalcolous *Peganum harmala* L., which was interpreted as evidence for the activation of an Fe deficiency response upon Pb

treatment (Mahdavian *et al.*, 2016). Furthermore, citrate may be directly involved in root-to-shoot Pb mobility. The concentration of Pb in xylem sap of Pb-treated cucumber (*Cucumis sativus* L.) was more than one order of magnitude larger when Fe was added to the nutrient solution as a citrate instead of as an EDTA complex (Tatár *et al.*, 1998).

Very little is known about uptake and translocation pathways for Pb in plants (Fasani *et al.*, 2018). Multivariate analysis of hundreds of paired soil–leaf samples had indicated a negative effect of soil Ca on leaf Pb accumulation (Stein *et al.*, 2017). Our competition experiments in hydroponic culture did not fully corroborate this finding. High external Ca reduced Pb accumulation only in the shoots of the accession with the highest Pb accumulation (Fig. S9). By contrast, root Pb concentrations were consistently reduced in the presence of Ca excess, whereas Zn excess had no such effect. This can be cautiously interpreted as suggesting an involvement of Ca transporters and apoplastic Ca-binding sites in the accumulation of Pb. This is in line with earlier reports on the protective effect of Ca against Pb toxicity in rice (Kim *et al.*, 2002) and the possible contribution of CNGC, AtCNGC1, AtCNGC11 and AtCNGC12 to Pb uptake in *A. thaliana* (Sunkar *et al.*, 2000; Moon *et al.*, 2019). Transcript analyses of candidate CNGCs identified in RNA-seq data sets for *A. thaliana* and two of the investigated *A. halleri* accessions (Table S2), however, did not reveal a consistent association of Pb uptake with elevated expression of *A. halleri* CNGC11 or CNGC12 relative to *A. thaliana* (Fig. S10).

After root-to-shoot translocation, metals are transferred to cells competent for storage and detoxification. For example, Zn allocation to leaf epidermal cells has been demonstrated for several Zn hyperaccumulating species (White & Pongrac, 2017). Interestingly, Zn allocation in *A. halleri* contrasts these reports, as it preferentially accumulates in leaf mesophyll cells (Küpper *et al.*, 2000; Zhao *et al.*, 2000; Sarret *et al.*, 2009). Our LA-ICP-MS data corroborate this finding (Fig. 7). Likewise, the strong accumulation of Zn and Cd observed at the base of the trichome by SEM-EDX (Fig. S15) concurs with previous reports on *A. halleri* (Küpper *et al.*, 2000; Zhao *et al.*, 2000). Much less information is available about Pb distribution. Strikingly, the strongest Pb accumulation in *A. halleri* was found in the petiole, followed by the leaf main vein and the leaf blade. This gradient was by contrast with that seen for Zn and may indicate lower cell-to-cell mobility of Pb away from the vasculature (Fig. S14). Within petioles and leaves, Pb was allocated to the epidermis and to cells within the vasculature, namely collenchyma cells, as suggested by the uneven thickness of the cell wall, and xylem elements (Figs 7, S13). The obvious contrast with the Zn distribution pattern in leaves suggests that accumulation pathways differ at least partially for Pb and Zn. This is further substantiated by the surprising finding that Pb did not co-localise with Zn and Cd at the bases of trichomes. Rather, it was concentrated in the symplast or apoplast of cells supporting the trichome (Fig. S15). Allocation of Pb to vasculature, but not to epidermis, was previously reported for a Zn and Cd hyperaccumulating ecotype of *S. alfredii*, where it co-localised with S but not with P (Tian *et al.*, 2010; Fig. S13). Predominant allocation of Pb to epidermis and

to abaxial collenchyma cells was also reported for field-collected *T. praecox* leaves (Vogel-Mikuš *et al.*, 2008a,b) and may be inferred from the Pb distribution in leaves of hydroponically grown *E. splendens* (Zhang *et al.*, 2011). The collenchyma cells are characterised by a pectin-rich cell wall, which may play a role in Pb binding. Pb allocation to the collenchyma cells, mechanically supporting the vein, indicates that these cells may serve as a disposal site for toxic heavy metals, thereby protecting sensitive and metabolically more active (and phloem-fed) tissues from metal toxicity (Vollenweider *et al.*, 2006; Vogel-Mikuš *et al.*, 2008a).

While Pb is a soft metal with high affinity to S, most reports have indicated storage of Pb in cell walls where S-containing molecules are scarce, making O-ligands of cell walls likely to be sites for Pb sorption. Our XANES analysis of *A. halleri* leaves supports this concept. Most Pb was assigned to the model Pb-acetate (Fig. 7). Pb-acetate is a representative bidentate ligand, which in form resembles the bidentate structure of Ca bound to homogalacturonan in the 'egg-box model'. Homogalacturonan is the most abundant structural class of pectic polysaccharides. Therefore, it would be sufficiently abundant to bind the supplied amount of Pb. As Ca^{2+} ions in homogalacturonan can be replaced by divalent heavy metal cations, we propose that this process takes place in *A. halleri* leaves. Using XANES, predominant binding of Pb to O-ligands in the cell wall has been reported for field-collected leaves, sampled from the vicinity of a Pb mine (Bovenkamp *et al.*, 2013) and in leaves of experimentally grown corn (Sun & Luo, 2018). Cell wall bound Pb was also found in the Cd and Zn hyperaccumulator *S. alfredii* (Tian *et al.*, 2010), as was strong apoplastic Pb binding to cell walls and intercellular spaces in *Vigna unguiculata* (L.) Walp. (Kopittke *et al.*, 2007). A smaller proportion of Pb was found either in octadentate coordination with SO_4 or in monoclinic coordination with PO_4 in *A. halleri* leaves, which was also supported by co-localisation of Pb and S and of Pb and P in the vasculature of petioles and leaves of *A. halleri* (Fig. S13). Furthermore, it is also in line with the co-localisation of Pb with S and PO_4 ligands for Pb in the Cd/Zn accumulating ecotype of *S. alfredii* (Tian *et al.*, 2010). Binding of Pb to sulfide-containing ligands was not supported when determining the best fits for the recorded spectra, making binding of Pb to proteins unlikely.

The field observations had already indicated opportunistic Pb accumulation by *A. halleri*, meaning accumulation occurs whenever Pb is phytoavailable due to particular soil conditions. Experiments reported here unequivocally showed Pb accumulation via uptake and *in planta* translocation. Furthermore, our results suggested a minor impact of genotype on Pb accumulation, which contrasted with a large genotype influence on Zn and Cd accumulation (Figs 1, 4) (Stein *et al.*, 2017).

Previously, sporadic detection of Pb in plant samples would have mostly been attributed to aerial deposition of particles. We propose instead that the comparatively erratic detection of Pb in above-ground tissues, for example relative to Cd or As, indicates that in most soils phytoavailability of Pb is low, which restricts

plant accumulation. However, when soil Pb becomes phytoavailable, plants will translocate at least a portion to the shoot. This was shown here with a focus on *A. halleri* (Figs 1, 2, 4). However, it is noteworthy that even *A. thaliana* grown on Bestwig soil or in hydroponics, that is under conditions in which Pb was phytoavailable, showed a considerable degree of leaf Pb accumulation ($95 \text{ mg kg}^{-1} \text{ DW}$; Fig. 2, $48 \text{ mg kg}^{-1} \text{ DW}$; Fig. 4, respectively) that represented on average *c.* 10–25% of the accumulation observed in *A. halleri*. Such levels would exert a food safety risk, if what we found for *A. thaliana* applies also to crop plants. Therefore, more studies on opportunistic Pb accumulation in other plant species are clearly needed.

Acknowledgements

This work was financially supported by the Deutsche Forschungsgemeinschaft (SPP1529 ADAPTOMICS, Cl152/9-1, -2; Kr1967/10-1, -2) to SC and UK and a postdoctoral fellowship by the Alexander von Humboldt foundation to PP. Financial support from the Slovenian Research Agency (ARRS) through programmes P1-0212, P1-0112 and I0-0005 and projects N7-077, J7-9418, J7-9398, N1-0105 and N1-0090 is gratefully acknowledged. ESRF, Grenoble, France, is acknowledged for provision of synchrotron radiation facilities at beamline BM23 for XANES analyses (project LS-2275). Dan Frost and Detlef Krauß from Bayerisches Geoinstitut, Bayreuth, Germany, are gratefully acknowledged for the SEM-EDX analysis. We thank Sina Fischer (University of Nottingham) for help with the speciation analysis, Yating Shen from the National Research Center for Geoanalysis, China, for providing the Pb-phosphate XANES spectrum and Christiane Meinen for expert technical assistance.

Author contributions

SH, PP, JTvE, MD, KVM, MB, MP, MW, BP, PV, PPe and IA performed experiments and data processing; SH, PP, UK and SC planned and designed the experiments; SH, PP and SC wrote the paper. All authors approved the final version of the paper. SH and PP contributed equally to this work.

ORCID

Iztok Arčon  <https://orcid.org/0000-0003-4333-4054>
Stephan Clemens  <https://orcid.org/0000-0003-0570-1060>
Ute Krämer  <https://orcid.org/0000-0001-7870-4508>
Matic Pečovnik  <https://orcid.org/0000-0001-5494-227X>
Primoz Pelicon  <https://orcid.org/0000-0003-2469-3342>
Björn Pietzenek  <https://orcid.org/0000-0002-2688-3783>
Paula Pongrac  <https://orcid.org/0000-0003-0721-7555>
Johannes T. van Elteren  <https://orcid.org/0000-0003-2237-7821>
Primoz Vavpetič  <https://orcid.org/0000-0001-6204-7435>
Katarina Vogel-Mikuš  <https://orcid.org/0000-0003-3430-1779>
Michael Weber  <https://orcid.org/0000-0001-5647-6217>

References

- Adriano DC. 2001. *Trace elements in terrestrial environments*. New York, NY, USA: Springer, New York.
- Álvarez-Fernández A, Díaz-Benito P, Abadía A, López-Millán A-F, Abadía J. 2014. Metal species involved in long distance metal transport in plants. *Frontiers in Plant Science* 5: 105.
- Baker AJM. 1981. Accumulators and excluders – strategies in the response of plants to heavy metals. *Journal of Plant Nutrition* 3: 643–654.
- Bovenkamp GL, Prange A, Schumacher W, Ham K, Smith AP, Hormes J. 2013. Lead uptake in diverse plant families: a study applying x-ray absorption near edge spectroscopy. *Environmental Science & Technology* 47: 4375–4382.
- Cook LL, McGonigle TP, Inouye RS. 2009. Titanium as an indicator of residual soil on arid-land plants. *Journal of Environmental Quality* 38: 188–199.
- Cornu J-Y, Deinlein U, Höreth S, Braun M, Schmidt H, Weber M, Persson DP, Husted S, Schjoerring JK, Clemens S. 2015. Contrasting effects of nicotianamine synthase knockdown on zinc and nickel tolerance and accumulation in the zinc/cadmium hyperaccumulator *Arabidopsis halleri*. *New Phytologist* 206: 738–750.
- Degryse F, Waegeneers N, Smolders E. 2007. Labile lead in polluted soils measured by stable isotope dilution. *European Journal of Soil Science* 58: 1–7.
- Dinh N, van der Ent A, Mulligan DR, Nguyen AV. 2018. Zinc and lead accumulation characteristics and *in vivo* distribution of Zn²⁺ in the hyperaccumulator *Noccaea caerulescens* elucidated with fluorescent probes and laser confocal microscopy. *Environmental and Experimental Botany* 147: 1–12.
- van der Ent A, Baker AJM, Reeves RD, Pollard AJ, Schat H. 2013. Hyperaccumulators of metal and metalloid trace elements: facts and fiction. *Plant and Soil* 362: 319–334.
- Fakhri Y, Bjørklund G, Bandpei AM, Chirumbolo S, Keramati H, Pouya RH, Asadi A, Amanidaz N, Sarafraz M, Sheikhmohammad A *et al.* 2018. Concentrations of arsenic and lead in rice (*Oryza sativa* L.) in Iran: a systematic review and carcinogenic risk assessment. *Food and Chemical Toxicology* 113: 267–277.
- Fasani E, Manara A, Martini F, Furini A, DalCorso G. 2018. The potential of genetic engineering of plants for the remediation of soils contaminated with heavy metals. *Plant, Cell & Environment* 41: 1201–1232.
- Fischer S, Kühnlenz T, Thieme M, Schmidt H, Clemens S. 2014. Analysis of plant Pb tolerance at realistic submicromolar concentrations demonstrates the role of phytochelatin synthesis for Pb detoxification. *Environmental Science and Technology* 48: 7552–7559.
- Heidari Dehno A, Mohtadi A. 2018. The effect of different iron concentrations on lead accumulation in hydroponically grown *Matthiola flavidula* Boiss. *Ecological Research* 33: 757–765.
- Hendershot WH, Duquette M. 1986. A simple barium chloride method for determining cation exchange capacity and exchangeable cations. *Soil Science Society of America Journal* 50: 605.
- Huang JW, Chen J, Berti WR, Cunningham SD. 1997. Phytoremediation of lead-contaminated soils: role of synthetic chelates in lead phytoextraction. *Environmental Science & Technology* 31: 800–805.
- Ilunga Kabeya F, Pongrac P, Lange B, Faucon MP, van Elteren JT, Šala M, Šelih VS, Vanden Eeckhoudt E, Verbruggen N. 2018. Tolerance and accumulation of cobalt in three species of *Haumaniastrum* and the influence of copper. *Environmental and Experimental Botany* 149: 27–33.
- Janssen RPT, Peijnenburg WJGM, Posthuma L, Van Den Hoop MAGT. 1997. Equilibrium partitioning of heavy metals in Dutch field soils. I. Relationship between metal partition coefficients and soil characteristics. *Environmental Toxicology and Chemistry* 16: 2470–2478.
- Kim Y-Y, Yang Y-Y, Lee Y. 2002. Pb and Cd uptake in rice roots. *Physiologia Plantarum* 116: 368–372.
- Klančnik K, Vogel-Mikuš K, Gaberščik A. 2014. Silicified structures affect leaf optical properties in grasses and sedge. *Journal of Photochemistry and Photobiology B: Biology* 130: 1–10.
- Kopittke PM, Asher CJ, Kopittke RA, Menzies NW. 2007. Toxic effects of Pb²⁺ on growth of cowpea (*Vigna unguiculata*). *Environmental Pollution* 150: 280–287.
- Kopittke PM, Asher CJ, Menzies NW. 2008. Prediction of Pb speciation in concentrated and dilute nutrient solutions. *Environmental Pollution* 153: 548–554.
- Kopittke PM, Blamey FPC, Asher CJ, Menzies NW. 2010. Trace metal phytotoxicity in solution culture: a review. *Journal of Experimental Botany* 61: 945–954.
- Koubová K, Tlustoš P, Břendová K, Száková J, Najmanová J. 2016. Lead accumulation ability of selected plants of *Noccaea* spp. *Soil and Sediment Contamination* 25: 882–890.
- Krämer U. 2010. Metal hyperaccumulation in plants. *Annual Review of Plant Biology* 61: 517–534.
- Küpfer H, Lombi E, Zhao F-J, McGrath SP. 2000. Cellular compartmentation of cadmium and zinc in relation to other elements in the hyperaccumulator *Arabidopsis halleri*. *Planta* 212: 75–84.
- Mahdavian K, Ghaderian SM, Schat H. 2016. Pb accumulation, Pb tolerance, antioxidants, thiols, and organic acids in metallophilous and non-metallophilous *Peganum harmala* L. under Pb exposure. *Environmental and Experimental Botany* 126: 21–31.
- Marx SK, Rashid S, Stromsoe N. 2016. Global-scale patterns in anthropogenic Pb contamination reconstructed from natural archives. *Environmental Pollution* 213: 283–298.
- McLaughlin MJ, Smolders E, Degryse F, Rietra R. 2011. Uptake of metals from soil into vegetables. In: Swartjes FA, ed. *Dealing with contaminated sites*. Glen Osmond, SA, Australia: Univ Adelaide, CSIRO Land and Water, 325–367.
- Menzies NW, Donn MJ, Kopittke PM. 2007. Evaluation of extractants for estimation of the phytoavailable trace metals in soils. *Environmental Pollution* 145: 121–130.
- Mišljenović T, Jakovljević K, Jovanović S, Mihailović N, Gajić B, Tomović G. 2018. Micro-edaphic factors affect intra-specific variations in trace element profiles of *Noccaea praecox* on ultramafic soils. *Environmental Science and Pollution Research* 25: 31737–31751.
- Mohtadi A, Ghaderian SM, Schat H. 2012a. A comparison of lead accumulation and tolerance among heavy metal hyperaccumulating and non-hyperaccumulating metallophytes. *Plant and Soil* 352: 267–276.
- Mohtadi A, Ghaderian SM, Schat H. 2012b. Lead, zinc and cadmium accumulation from two metalliferous soils with contrasting calcium contents in heavy metal-hyperaccumulating and non-hyperaccumulating metallophytes: a comparative study. *Plant and Soil* 361: 109–118.
- Mohtadi A, Ghaderian SM, Schat H. 2013. The effect of EDDS and citrate on the uptake of lead in hydroponically grown *Matthiola flavidula*. *Chemosphere* 93: 986–989.
- Moon JY, Belloeil C, Ianna ML, Shin R. 2019. Arabidopsis CNGC family members contribute to heavy metal ion uptake in plants. *International Journal of Molecular Sciences* 20: 413.
- Norton GJ, Deacon CM, Mestrot A, Feldmann J, Jenkins P, Baskaran C, Meharg AA. 2015. Cadmium and lead in vegetable and fruit produce selected from specific regional areas of the UK. *Science of the Total Environment* 533: 520–527.
- Norton GJ, Williams PN, Adomako EE, Price AH, Zhu Y, Zhao FJ, McGrath S, Deacon CM, Villada A, Sommella A *et al.* 2014. Lead in rice: analysis of baseline lead levels in market and field collected rice grains. *Science of the Total Environment* 485–486: 428–434.
- Pilon-Smits EAH. 2017. Mechanisms of plant selenium hyperaccumulation. In: Pilon-Smits EAH, Winkel LHE, Lin Z-Q, eds. *Selenium in plants: molecular, physiological, ecological and evolutionary aspects*. Cham, Switzerland: Springer International Publishing, 53–66.
- Pollard AJ, Reeves RD, Baker AJM. 2014. Facultative hyperaccumulation of heavy metals and metalloids. *Plant Science* 217: 8–17.
- Pongrac P, Scheers N, Sandberg A-S, Potisek M, Arcon I, Kreft I, Kump P, Vogel-Mikuš K. 2016. The effects of hydrothermal processing and germination on Fe speciation and Fe bioaccessibility to human intestinal Caco-2 cells in Tartary buckwheat. *Food Chemistry* 199: 782–790.
- Pongrac P, Vogel-Mikuš K, Kump P, Nečemer M, Tolrà R, Poschenrieder C, Barceló J, Regvar M. 2007. Changes in elemental uptake and arbuscular mycorrhizal colonisation during the life cycle of *Thlaspi praecox* Wulfen. *Chemosphere* 69: 1602–1609.
- Ravel B, Newville M. 2005. ATHENA, ARTEMIS, HEPHAESTUS: data analysis for X-ray absorption spectroscopy using IFEFFIT. *Journal of Synchrotron Radiation* 12: 537–541.

- Reeves RD, Baker AJM, Jaffré T, Erskine PD, Echevarria G, van der Ent A. 2018. A global database for plants that hyperaccumulate metal and metalloids trace elements. *New Phytologist* 218: 407–411.
- Ryan CG. 2000. Quantitative trace element imaging using PIXE and the nuclear microprobe. *International Journal of Imaging Systems and Technology* 11: 219–230.
- Saifullah Meers E, Qadir M, de Caritat P, Tack FMG, Du Laing G, Zia MH. 2009. EDTA-assisted Pb phytoextraction. *Chemosphere* 74: 1279–1291.
- Sarret G, Willems G, Isaure M-P, Marcus MA, Fakra SC, Frérot H, Pairis S, Geoffroy N, Manceau A, Saumitou-Laprade P. 2009. Zinc distribution and speciation in *Arabidopsis halleri* × *Arabidopsis lyrata* progenies presenting various zinc accumulation capacities. *New Phytologist* 184: 581–595.
- Sauvé S, Martínez CE, McBride M, Hendershot W. 2000. Adsorption of free lead (Pb) by pedogenic oxides, ferrihydrite, and leaf compost. *Soil Science Society of America Journal* 64: 595.
- Sauvé S, McBride M, Hendershot W. 1998. Lead phosphate solubility in water and soil suspensions. *Environmental Science & Technology* 32: 388–393.
- Schreck E, Foucault Y, Sarret G, Sobanska S, Cécillon L, Castrec-Rouelle M, Uzu G, Dumat C. 2012. Metal and metalloids foliar uptake by various plant species exposed to atmospheric industrial fallout: mechanisms involved for lead. *Science of the Total Environment* 427–428: 253–262.
- Schuler M, Rellán-Álvarez R, Fink-Straube C, Abadía J, Bauer P. 2012. Nicotianamine functions in the phloem-based transport of iron to sink organs, in pollen development and pollen tube growth in *Arabidopsis*. *Plant Cell* 24: 2380–2400.
- Schwartzman MS, Corso M, Fataftah N, Scheepers M, Nouet C, Bosman B, Carnol M, Motte P, Verbruggen N, Hanikenne M. 2018. Adaptation to high zinc depends on distinct mechanisms in metalicolous populations of *Arabidopsis halleri*. *New Phytologist* 218: 269–282.
- Shen Y. 2014. Distribution and speciation of lead in model plant *Arabidopsis thaliana* by synchrotron radiation X-ray fluorescence and absorption near edge structure spectrometry. *X-Ray Spectrometry* 43: 146–151.
- Stein RJ, Höreth S, de Melo JRF, Syllwasschy L, Lee G, Garbin ML, Clemens S, Krämer U. 2017. Relationships between soil and leaf mineral composition are element-specific, environment-dependent and geographically structured in the emerging model *Arabidopsis halleri*. *New Phytologist* 213: 1274–1286.
- Sun J, Luo L. 2018. Subcellular distribution and chemical forms of Pb in corn: strategies underlying tolerance in Pb stress. *Journal of Agricultural and Food Chemistry* 66: 6675–6682.
- Sunkar R, Kaplan B, Bouché N, Arazi T, Dolev D, Talke IN, Maathuis FJ, Sanders D, Bouchez D, Fromm H. 2000. Expression of a truncated tobacco NtCBP4 channel in transgenic plants and disruption of the homologous *Arabidopsis* CNGC1 gene confer Pb²⁺ tolerance. *The Plant Journal* 24: 533–542.
- Tatár E, Mihucz VG, Varga A, Zárny Gy, Fodor F. 1998. Determination of organic acids in xylem sap of cucumber: effect of lead contamination. *Microchemical Journal* 58: 306–314.
- Tian S, Lu L, Yang X, Webb SM, Du Y, Brown PH. 2010. Spatial imaging and speciation of lead in the accumulator plant *Sedum alfredii* by microscopically focused synchrotron x-ray investigation. *Environmental Science & Technology* 44: 5920–5926.
- Villafort Carvalho MT. 2016. *Gomphrena clausenii*, a Zn and Cd hyperbioindicator species. PhD dissertation, Wageningen University, Wageningen, the Netherlands.
- Vogel-Mikuš K, Drobne D, Regvar M. 2005. Zn, Cd and Pb accumulation and arbuscular mycorrhizal colonisation of pennycress *Thlaspi praecox* Wulf. (Brassicaceae) from the vicinity of a lead mine and smelter in Slovenia. *Environmental Pollution* 133: 233–242.
- Vogel-Mikuš K, Pongrac P, Kump P, Nečemer M, Regvar M. 2006. Colonisation of a Zn, Cd and Pb hyperaccumulator *Thlaspi praecox* Wulfen with indigenous arbuscular mycorrhizal fungal mixture induces changes in heavy metal and nutrient uptake. *Environmental Pollution* 139: 362–371.
- Vogel-Mikuš K, Pongrac P, Pelicon P. 2014. Micro-PIXE elemental mapping for ionome studies of crop plants. *International Journal of PIXE* 24: 217–233.
- Vogel-Mikuš K, Regvar M, Mesjasz-Przybyłowicz J, Przybyłowicz WJ, Simčić J, Pelicon P, Budnar M. 2008a. Spatial distribution of cadmium in leaves of metal hyperaccumulating *Thlaspi praecox* using micro-PIXE. *New Phytologist* 179: 712–721.
- Vogel-Mikuš K, Simčić J, Pelicon P, Budnar M, Kump P, Nečemer M, Mesjasz-Przybyłowicz J, Przybyłowicz WJ, Regvar M. 2008b. Comparison of essential and non-essential element distribution in leaves of the Cd/Zn hyperaccumulator *Thlaspi praecox* as revealed by micro-PIXE. *Plant, Cell & Environment* 31: 1484–1496.
- Vollenweider P, Cosio C, Günthardt-Goerg MS, Keller C. 2006. Localization and effects of cadmium in leaves of a cadmium-tolerant willow (*Salix viminalis* L.). Part II microlocalization and cellular effects of cadmium. *Environmental and Experimental Botany* 58: 25–40.
- Wang H, Lu S, Li H, Yao Z. 2007. EDTA-enhanced phytoremediation of lead contaminated soil by *Bidens maximowicziana*. *Journal of Environmental Sciences* 19: 1496–1499.
- White PJ, Brown PH. 2010. Plant nutrition for sustainable development and global health. *Annals of Botany* 105: 1073–1080.
- White PJ, Pongrac P. 2017. Heavy metal toxicity in plants. In: Shabala S, ed. *Plant stress physiology*. Wallingford, UK: CABI, 300–331.
- Zhang J, Tian S, Lu L, Shohag MJ, Liao H, Yang X. 2011. Lead tolerance and cellular distribution in *Elsholtzia splendens* using synchrotron radiation micro-X-ray fluorescence. *Journal of Hazardous Materials* 197: 264–271.
- Zhao FJ, Adams ML, Dumont C, McGrath SP, Chaudri AM, Nicholson FA, Chambers BJ, Sinclair AH. 2004. Factors affecting the concentrations of lead in British wheat and barley grain. *Environmental Pollution* 131: 461–468.
- Zhao FJ, Lombi E, Brendon T, McGrath SP. 2000. Zinc hyperaccumulation and cellular distribution in *Arabidopsis halleri*. *Plant, Cell & Environment* 23: 507–514.

Supporting Information

Additional Supporting Information may be found online in the Supporting Information section at the end of the article.

Fig. S1 Original locations of *Arabidopsis halleri* accessions used in the experiments.

Fig. S2 Growth of *Arabidopsis halleri* in native metalliferous soil.

Fig. S3 Ionome profiles of *Arabidopsis halleri* and *A. thaliana* after cultivation in native metalliferous soil.

Fig. S4 Shoot metal accumulation dependent on soil exchangeable metal.

Fig. S5 Shoot biomass of *Arabidopsis halleri* and *A. thaliana* after cultivation in a metal gradient in native metalliferous soil.

Fig. S6 Mineral nutrition in *Arabidopsis halleri* shoots after cultivation in metal gradient in native metalliferous soil.

Fig. S7 Growth response of *Arabidopsis thaliana* Col-0 individuals to Pb²⁺ exposure in hydroponic culture.

Fig. S8 Mineral element response in Pb-treated *Arabidopsis halleri*.

Fig. S9 Accumulation of lead (Pb), zinc (Zn) and iron (Fe) in shoots and roots of hydroponically grown *Arabidopsis halleri* plants, depending on increased calcium (Ca) and Zn supply.

Fig. S10 Transcript abundance of candidate *CNGC* genes in roots and shoots of *A. thaliana* and three *A. halleri* accessions.

Fig. S11 Ratios of element concentrations in xylem sap.

Fig. S12 Changes in xylem sap metabolite profiles of *A. halleri* plants upon Pb exposure.

Fig. S13 Spatial distribution of phosphorus (P), sulphur (S), potassium (K), calcium (Ca), zinc (Zn) and lead (Pb) in leaves of *Arabidopsis halleri*.

Fig. S14 Metal accumulation in different parts of shoots of hydroponically grown *Arabidopsis halleri*.

Fig. S15 Spatial distribution of Ca (Ca), cadmium (Cd), lead (Pb) and zinc (Zn) in trichomes of *Arabidopsis halleri*.

Methods S1 Detailed methods.

Table S1 Theoretical lead (Pb) availability in the low phosphate, low pH hydroponic nutrient solution as estimated using the VISUALMINTEQ 3.1 program.

Table S2 Significantly differentially expressed *CNGC* genes identified by RNA-seq.

Table S3 Complete list of the metabolites detected in the xylem sap of *A. halleri* and the accompanying statistics.

Table S4 Average theoretical lead (Pb) species in xylem sap of *A. halleri* accessions.

Please note: Wiley-Blackwell are not responsible for the content or functionality of any supporting information supplied by the authors. Any queries (other than missing material) should be directed to the *New Phytologist* Central Office.



About New Phytologist

- *New Phytologist* is an electronic (online-only) journal owned by the New Phytologist Trust, a **not-for-profit organization** dedicated to the promotion of plant science, facilitating projects from symposia to free access for our Tansley reviews and Tansley insights.
- Regular papers, Letters, Research reviews, Rapid reports and both Modelling/Theory and Methods papers are encouraged. We are committed to rapid processing, from online submission through to publication 'as ready' via *Early View* – our average time to decision is <26 days. There are **no page or colour charges** and a PDF version will be provided for each article.
- The journal is available online at Wiley Online Library. Visit **www.newphytologist.com** to search the articles and register for table of contents email alerts.
- If you have any questions, do get in touch with Central Office (np-centraloffice@lancaster.ac.uk) or, if it is more convenient, our USA Office (np-usaoffice@lancaster.ac.uk)
- For submission instructions, subscription and all the latest information visit **www.newphytologist.com**